Journal of Physiology (1991), **443**, *pp.* 307–334
With 12 figures
Printed in Great Britain

GATING OF L-TYPE Ca^{2+} CHANNELS IN EMBRYONIC CHICK VENTRICLE CELLS: DEPENDENCE ON VOLTAGE, CURRENT AND CHANNEL DENSITY

BY MICHELE MAZZANTI*, LOUIS J. DEFELICE AND YUAN-MOU LIU‡

From the Department of Anatomy and Cell Biology, Emory University School of Medicine, Atlanta, GA 30322, USA

(*Received 11 September 1990*)

SUMMARY

1. L-type calcium channels in embryonic chick heart ventricle have voltage-dependent, time-variant kinetics when they conduct inward currents carried by 20 mM-Ba^{2+}. Depolarizing the membrane from −20 to 20 mV increases mean open time from 1·4 to 4·2 ms. Mean open time increases monotonically with voltage. The single-channel conductance, 18 ± 2 pS, is approximately linear over this voltage range, and the extrapolated reversal potential is 38 ± 5 mV.

2. In cell-attached patches with five or more L-type Ca^{2+} channels in the patch, the currents elicited by 500 ms depolarizing steps, from a −80 mV holding potential, inactivate rapidly and have large tail currents. In the same patch, currents from a −40 mV holding potential are smaller, inactivate more slowly, and have practically no tail currents.

3. In cell-attached patches containing one of two L-type Ca^{2+} channels, currents from −80 or −40 mV are virtually identical, and they are similar to the currents from multichannel patches held at −40 mV.

4. The voltage-dependent, time-variant kinetics of individual L-type Ca^{2+} channels are unaltered if the patch is removed from the cell and forms an inside-out configuration. In these experiments the internal membrane was bathed with an artificial, intracellular-like solution containing no phosphorylating enzymes or substrates.

5. Cells bathed in 20 mM-Ba^{2+} solutions and held at −80 mV have currents with an early phase that inactivates in tens of milliseconds, a late phase that inactivates in hundreds of milliseconds, and a large, slow tail current. Currents from −40 mV have only the late phase and practically no tails. However, if the maximum current is less than 0·1 pA pF^{-1}, records from either −80 or −40 mV are virtually identical, and they are similar to currents from cells with higher channel density held at −40 mV. Furthermore, if cells are stimulated before full recovery from inactivation, the reduced current is accompanied by slower inactivation.

* Present Address: Fisiologia e Biochemica Generale, Via Celoria 26, 20133 Milano, Italy.
‡ Present Address: Department of Physiology, Shanghai Second Medical University, Shanghai 200025, Peoples Republic of China.

MS 8793

6. Whole-cell currents in 1·5 mM-Ca^{2+} solutions are entirely abolished by addition of 20 μM-nifedipine, and they are enhanced 2-3 times by addition of 30 μM-cyclic AMP and 3 mM-ATP to the whole-cell recording electrode. The whole-cell currents in 20 mM-Ba^{2+} solutions are also completely blocked by 20 μM-nifedipine, regardless of kinetics or holding potential. Thus, by definition, the cells we are studying contain only L-type channels.

7. A model of L-type Ca^{2+} channels that accounts for the essential features of these data includes a voltage-dependent inactivated state and a current-dependent blocked state. The probability that a channel is in the blocked state is proportional to the number of ions that pass through it less the number that leak away. The model assumes that ions crossing a particular channel may block adjacent pores. Such a mechanism explains the rapid 'inactivation' kinetics of L-type Ca^{2+} currents that develop if channel density is sufficiently high.

INTRODUCTION

One of the earliest indications that internal free Ca^{2+} plays a critical role in excitability is from Hagiwara & Nakajima (1966), who showed that when they elevated internal Ca^{2+} to 5×10^{-7} M, they abolished action potentials in perfused barnacle muscle fibres. This phenomenon was later interpreted as Ca^{2+}-induced inactivation of Ca^{2+} channels, a mechanism that was studied by Brehm & Eckert (1978) and Brehm, Eckert & Tillotson (1980) in *Paramecium*; transient inward currents relaxed more slowly after they injected EGTA and were followed by a steady inward current; when they interrupted Ca^{2+} entry they interfered with inactivation, whereas when they enhanced entry, or otherwise increased the intracellular Ca^{2+}, they promoted inactivation. Chad & Eckert (1984) calculated that incomplete buffering in the cytoplasm may limit the dispersion of Ca^{2+} ions that enter the cell, and thus create Ca^{2+} domains near Ca^{2+} channels. According to these authors, the Ca^{2+} domains associated with individual pores could explain Ca^{2+}-dependent inactivation.

Ca^{2+}-mediated inactivation of L-type Ca^{2+} current occurs in cardiac cells (Kohlhardt, Krause, Kubler & Herdey, 1975; Hume & Giles, 1983; Josephson, Sanchez-Chapula & Brown, 1984; Mentrard, Vassort & Fischmeister, 1984; Lee, Marban & Tsien, 1985; Argibay, Fischmeister & Hartzell, 1988). Argibay *et al.* worked on adult frog ventricle cells, where the peak currents varied between 1·3 to 28 pA pF^{-1} from cell to cell. They showed that the lower the current density the higher the fraction of Ca^{2+} channels that are able to respond to a voltage challenge. Moreover, when they elevated the Ca^{2+} current by cyclic AMP (5 μM increased it 6- to 7- fold), they decreased the available current. Their results support the idea that the number of active Ca^{2+} channels per unit area diminishes the availability of channels to a voltage challenge. Ca^{2+}-mediated inactivation and voltage-dependent inactivation both exist in cardiac cells, and Ca^{2+}-mediated inactivation appears to function, though less effectively, if Ba^{2+} replaces Ca^{2+} as the charge carrier (Kass & Sanguinetti, 1984; Bean, 1985; McDonald, Cavalie, Trautwein & Pelzer, 1986; Campbell, Giles & Shibata, 1988*a*; Hirano, January & Fozzard, 1989; Hartzell & White, 1989).

If the current through a particular pore blocks not only the current through that

channel but also adjacent pores, one might expect that higher densities of channels would speed up the declining phase of L-type currents. To test this hypothesis we took advantage of the variability in Ca^{2+} channel density in ventricle cells from 7-day-old chick embryo hearts. Cell-attached patches on these cells typically contain one to ten channels. By comparing the currents from different patches we explored the relationship between channel density and channel kinetics. In this study we used solutions that contained 20 mM-Ba^{2+} to generate single-channel events large enough to be easily detected above background noise (Reuter, Stevens, Tsien & Yellen, 1982; Tsien, Bean, Hess & Nowycky, 1983; Cavalie, Ochi, Pelzer & Trautwein, 1983). Ba^{2+} also reduces I_{K1} (inward rectifying) current, which is common in our tissue (Mazzanti & DeFelice, 1988; Mazzanti & DeFelice, 1990*a*); if present, I_{K1} currents would be difficult to separate from Ca^{2+} currents in the patch and whole-cell recordings and would therefore interfere with the analysis of the Ca^{2+} currents.

In a previous study on cardiac cells we showed that single L-type Ca^{2+} channels, when conducting current in 10 mM-Ba^{2+} solutions, vary their kinetics smoothly over a narrow voltage range: at −20 mV openings are brief, low probability events; at 20 mV the openings are longer and they occur more frequently (Mazzanti & DeFelice, 1990*b*). In the present study we confirm this result and extend it to include the influence of channel density on L-type channel kinetics. Ba^{2+} currents through L-type Ca^{2+} channels inactivate only slightly during the 500 ms after a voltage step, regardless of holding potential. Furthermore, these voltage-dependent kinetics are unaltered in inside-out patches even when we expose the internal membrane to solutions free of phosphorylating enzymes or substrates. However, when the patch contains five or more channels, the Ba^{2+} currents are not only larger, as would be expected, but they also decline more rapidly. This decrease is evident when we hold the patch at −80 mV, but it is virtually absent when we hold it at −40 mV. Thus the kinetics of L-type Ca^{2+} channels do depend on channel density. If the channels are voltage inactivated, however, the influence of density is attenuated. The single-channel data correlate with the whole-cell experiments performed in 20 mM-Ba^{2+} solutions. In cells with sufficiently high current density, a marked difference exists between currents elicited from −80 or −40 mV holding potentials, but in cells with densities below 0·1 pA pF^{-1}, this dependence on holding potential vanishes. In addition, if we reduce the current by stimulating cells before they recover from inactivation, the speed of the apparent inactivation is also reduced.

We interpreted these results by a model in which L-type Ca^{2+} channels exhibit both voltage-dependent inactivation and current-dependent block. The current-dependent block manifests itself through ions that accumulate after they pass through a channel. One or two channels in a patch are insufficient for current-dependent block at voltages between −20 and 20 mV. However, it is conceivable that voltages which evoke higher currents, or currents elicited in higher concentrations of Ba^{2+} or Ca^{2+} might also show current-dependent block in an isolated channel. A recent paper by Yue, Backx & Imredy, (1991) shows that individual channels in which currents are elicited in the presence of 160 mM-Ca^{2+} modulate their own gating, but currents in 160 mM-Ba^{2+} do not. In our experiments in 20 mM-Ba^{2+} solution, five or more channels are required in a patch to block the current. The model we use requires that each channel interact with all the ions flowing into the patch; that is, the rate constant to the blocked state is proportional to the total

current from n channels. When applying the model to a cell, the apparent assumption is that all n channels in the cell are uniformly distributed. However, the hypothesis does not require this postulate. One could imagine more complex models in which only a fraction of the channels were uniformly distributed while the rest occurred in more dense clusters. In this case the rate constant to the blocked state ought to be proportional only to the numbers of channels in the clusters. The total current would be the uniform, low-density currents plus the clustered, high-density currents. This point of view has several attractive features; however, without additional information an explicit model along these lines is unwarranted. Holding at -80 mV increases the probability that a channel will be active, thus generating a large blocking current. Holding at -40 mV increases inactivation, which diminishes the available current and the subsequent block. To a limited extent the effects of holding potential are mimicked by low channel density and incomplete recovery from inactivation.

METHODS

Embryonic ventricle cells were prepared by enzymatic digestion of 7-day-old chick embryo hearts (Fujii, Ayer & DeHaan, 1988). After the cells were in tissue culture medium 12–24 h, and immediately preceding the experiments, we washed the cells with bath solution at room temperature. The composition of the bath solution in mM units was: 130 NaCl, 1·3 KPO_4, 1·5 $CaCl_2$, 0·5 $MgSO_4$, 5 dextrose, 10 HEPES, adjusted to 7·35 pH and 273 mosM. The cell-attached electrode solution for measuring patch currents contained (in mM): 20 $BaCl_2$, 110 NaCl, 1·3 KPO_4, 0·5 $MgSO_4$, 5 EGTA, 0·01 tetrodotoxin (TTX), 5 tetraethylammonium (TEA), 10 4-aminopyridine (4-AP), 10 HEPES, 5 dextrose, adjusted to 7·35 pH and 273 mosM. The cell-detached electrode contained the 20 mM-Ba^{2+} solution; however, in those experiments in which we compared patches before and after they were ripped off, the bath solution was identical to our whole-cell electrode solution (Mazzanti & DeFelice, 1990*b*). This whole-cell solution consisted of (in mM): 120 KCl, 0·1 $CaCl_2$, 2 $MgCl_2$, 1·1 EGTA, 10 HEPES, adjusted to 7·35 pH and 268 mosM; thus, the internal surface of the membrane faces an intracellular-like solution, free of phosphorylating enzymes or substrates. The Ba^{2+} ions increase the conductance of L-type Ca^{2+} channels (Cavalie *et al.* 1983; Nilius, Hess, Lansman & Tsien, 1985; Hess, Lansman & Tsien, 1984, 1986; Yue & Marban, 1990), and they reduce contamination by I_{K1} currents (inward rectifier). Ba^{2+} does not eliminate I_{K1} completely. Therefore, after forming a patch, we quickly examined it for I_{K1} channels by hyperpolarizing the patch, and we eliminated patches that contained inward-rectifier channels or that had excessive noise (Mazzanti & DeFelice, 1988).

The patch electrodes were made from borosilicate glass (Corning 7052), drawn on a programmable puller (Sachs-Flaming PC-84, Sutter Instruments San Rafael, CA, USA). After we coated the tip with Sylgard (Dow Corning), fire-polished the tip to approximately 1 μm internal diameter, and filled the electrodes with the 20 mM-Ba^{2+} solution, the electrodes had resistances of around 6 MΩ. The estimated surface area of the patch formed with these electrodes, calculated from geometric considerations and capacitive measurements (Mazzanti & DeFelice, 1987*a*, *b*; Wellis, DeFelice & Mazzanti, 1990) is between 5 and 7 μm_2. The lower limit of the patch membrane capacitance, about 0·07 pF, is only achieved in one-electrode experiments because of cross-talk between electrodes in two-electrode experiments (Mazzanti & DeFelice, 1987*a*, *b*). In the present study the small variation in capacitance from patch to patch indicates a constant patch area to within $\pm 20\%$. Thus we attribute the variable number of channels in patches formed on 7-day-old chick ventricle cells to variable (or heterogeneous) channel density rather than inconsistent patch area. For the present experiments we selected patches in which the leak conductance of the patch membrane was extremely low. In previous experiments we measured leak conductance of the patch membrane by an iteration routine, in which we fitted evoked patch current to an equation of the form $c(dV/dt)+gV+i_0$, where c is patch capacitance, g is patch conductance, and i_0 is baseline current (Wellis *et al.* 1990). Although we did not apply this routine to each patch, the low noise levels of the patches we elected to study indicated resistive leak pathways greater than 250 GΩ. The cells

we used were about 10–13 μm in diameter and had conductances of about 1–10 GΩ. In some experiments we used small clusters of two or three small cells joined together. (See Results, Fig. 8.)

The current was measured with a List EPC-7 amplifier (Darmstadt, Germany). The data were band-limited at 1000 Hz for analysis, and we subtracted the capacitive transient from all traces. Amplitude histograms were calculated by sampling the data every 0·2 ms. For a more detailed description of the recording technique, see Mazzanti & DeFelice (1987*a*, *b*, 1988, 1990*a*, *b*) and Wellis *et al.* (1990). In the cell-attached patch experiments we voltage clamped the patch pipette to various potentials and measured the cell resting potential afterwards by breaking the patch. We assumed that the voltage first recorded after the rupture corresponded to the potential before the break. This procedure has been verified in two-electrode experiments (Mazzanti & DeFelice, 1987*a*, *b*). The difference between the resting potential and the pipette potential was taken as the voltage across the patch membrane. This is the voltage plotted in the figures. In whole-cell experiments we voltage-clamped the cell in the usual manner; in inside-out patch experiments the bath was ground and the membrane potential was simply the negative of the pipette potential; e.g. to obtain a membrane potential of $V = -20$ mV, we applied a pipette potential of $V_p = +20$ mV. We stored the data on a VCR and analysed them after the experiments on a Nicolet 4094 oscilloscope and an IBM-AT computer, using programs developed by William N. Goolsby. The modelling was done with a program called MACROCHAN, which was also developed 'in house' and is available on request (DeFelice, Goolsby & Huang, 1985).

RESULTS

Figure 1*A* illustrates a voltage-clamp experiment on a cell-attached patch. The cell was in bath solution while the patch was exposed to the 20 mM-Ba^{2+} solution. The indicated voltages are the absolute potentials of the patch membrane. In a relatively narrow range of voltages, the kinetics change from long openings to brief, low probability openings. At 20 mV the channel is virtually open throughout the 500 ms test potential, although it flickers to the closed state repeatedly; at -20 mV the channel is open for a small fraction of the pulse duration. The closed state corresponds to the dash indicating 0 pA, and the open state corresponds to some negative current. The distribution between these two states depends on the filter setting (100 Hz for these data). To quantify this distribution we calculated the amplitude histograms in Fig. 1*B*, for 3·2 s of data at each potential. In each frame the peak at 0 pA represents the closed state and the peak to the left represents the open state. The off-set currents have been subtracted. The histograms indicate that the average probability of channels being open changes gradually with membrane depolarization.

Figure 2 summarizes data from five separate experiments, in which each patch contained just one channel. The graph in the upper half of the figure is the open state probability P_o as a function of membrane voltage. Every point represents the Gaussian area of the open state relative to total area of the open-plus-closed-state histograms. The continuous line is a non-linear least-squares fit to the equation:

$$P_o = 0{\cdot}7 \exp a(V-b)/[1+\exp a(V-b)],$$

where $a = 0{\cdot}09$/mV and $b = -3{\cdot}75$ mV. The graph in the lower quadrants is the open channel i–V curve. Each point and bar represents the average current and the average standard deviation from open-state histograms of the separate experiments. The straight line is a linear least-squares fit to the equation:

$$i = \gamma(V-E),$$

where $\gamma = 18$ pS and $E = 38$ mV.

The patch illustrated in Fig. 3 contains at least five channels. The raw data in each current trace show the response to five consecutive steps to the same test potential; each 500 ms step is actually separated by a 1 s interval not shown. The experiment was repeated for four test potentials. When the holding potential is −80 mV, the

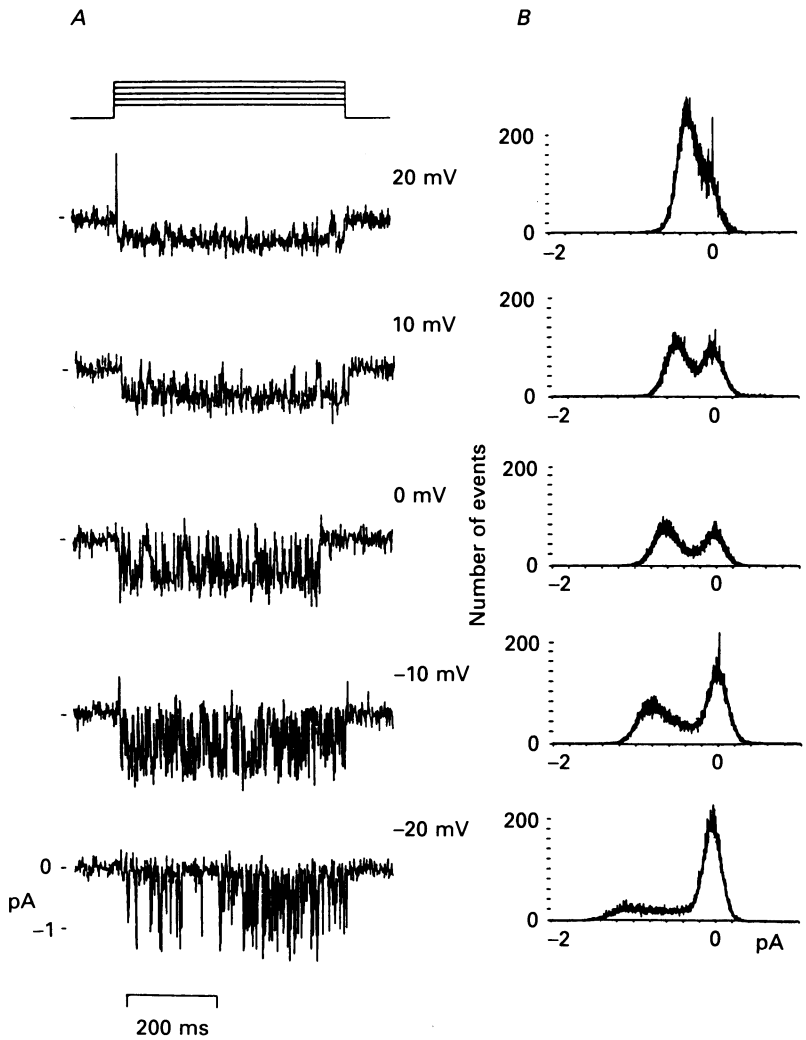

Fig. 1. *A*, current–voltage characteristics of a single L-type Ca^{2+} channel isolated in a cell-attached patch on a 7-day-old chick ventricle cell. The cell was in normal physiological saline at room temperature; the patch solution contained 20 mM-Ba^{2+}. Records without tail currents were selected for this figure. The resting potential of the cell (−80 mV) was measured by breaking the patch at the end of the experiment. (For more details on solutions and resting potentials, see Methods.) The step protocols at the top of the panel are from a holding potential of −80 mV. They indicate the duration, sign, and absolute test voltage (shown beside each trace) experienced by the patch. *B*, amplitude histograms of 3·2 s of data at the indicated test potentials. Tail currents were edited from the data for histogram analysis. All current traces were filtered at 1000 Hz before analysis.

currents show a marked voltage-dependent decline during each 500 ms step. When the holding potentials is −40 mV, the number of active channels is reduced and the decline during each step is virtually absent. Figure 3*B* verifies that shifting the holding potential from −80 to −40 mV reduces the number of active channels, and

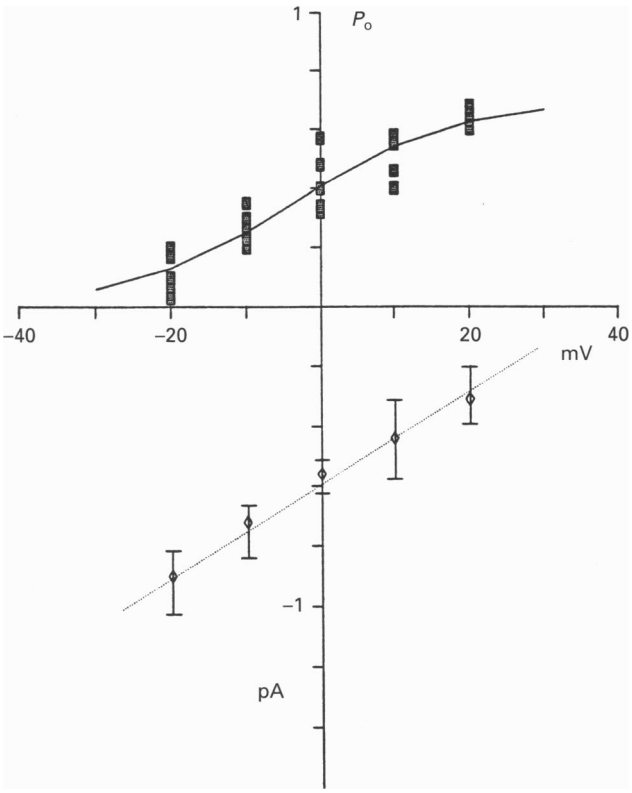

Fig. 2. Top, open-state probability as a function of membrane voltage (P_o–V), obtained by plotting the relative area under Gaussian fits to the histograms in Fig. 1*B* against the absolute membrane voltage at which the data were obtained. The five filled squares indicate separate experiments. The continuous line through the data points is a theoretical fit to the Boltzmann equation (see text). Bottom, open channel probability curve as a function of membrane voltage (i–V), obtained by plotting the average of the difference currents from the Gaussian fits to the histograms in Fig. 1*B versus* the absolute membrane potential. ◇ and error bars are average means and standard deviations from Gaussian fits to five experiments. The conductance of the channel in 20 mM-Ba^{2+} is 18±2 pS, and the reversal potential is 38±5 mV.

that all channels have the same conductance. The effect of holding potential is fully reversible.

Figure 4 repeats the experiment of Fig. 3 except that we selected a patch that contained only two Ca^{2+} channels. All other conditions were the same. As before we concatenated five consecutive traces and compared the results at different holding potentials. With two channels in the patch, the holding potential has little effect on the number of active channels, and the pronounced decay during each cycle is absent.

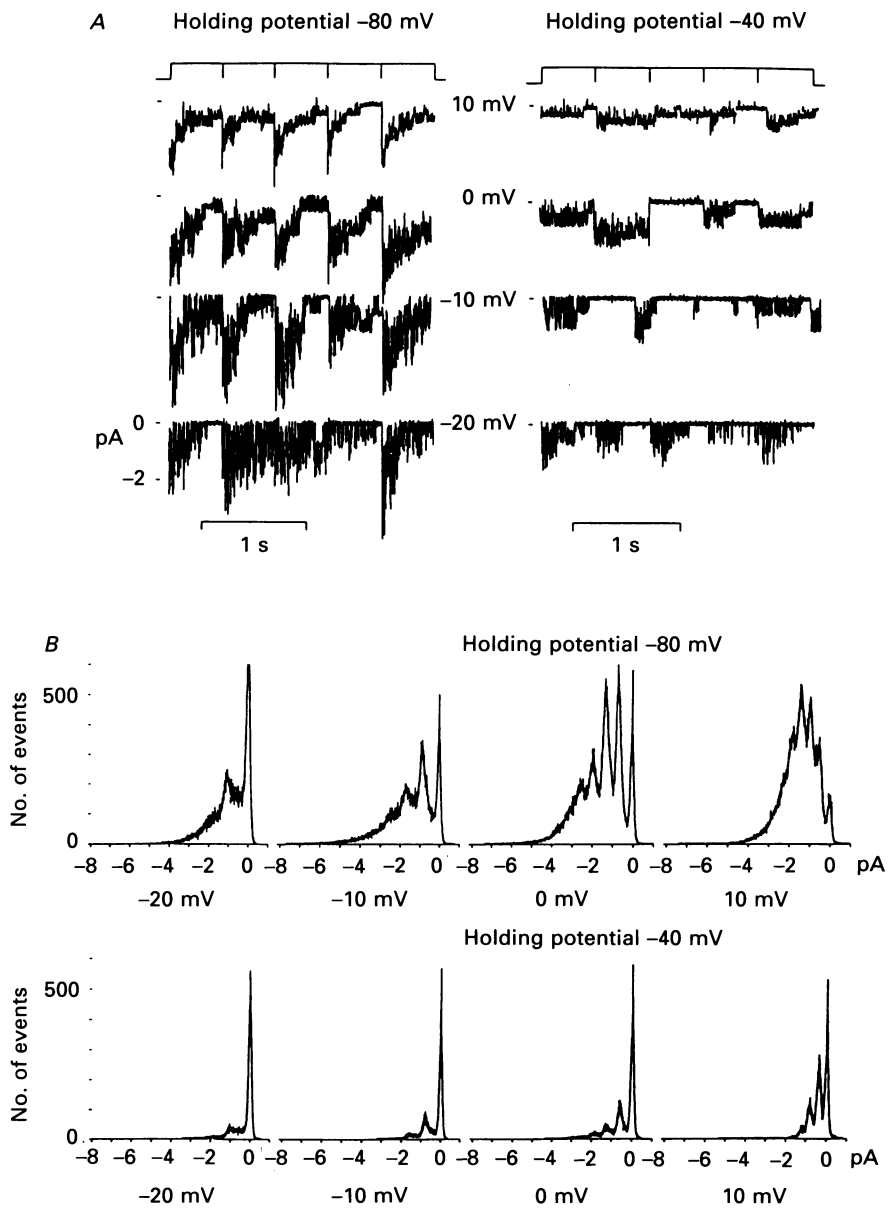

Fig. 3. *A*, examples of currents from a patch that contained at least five channels. In each trace we concatenated five responses to the indicated test potentials. The tail currents and the inter-test interval are suppressed. The pulses were actually separated by 1 s. The holding potential was either −80 or −40 mV. With five channels in the patch, holding at −40 mV reduces the number of active channels and practically eliminates the time-variant inactivation of channels, which is obvious from a holding potential of −80 mV. The effect of holding potential is fully reversible. *B*, amplitude histograms of the concatenated current traces. Note that at each test potential, the separations between current peaks are equal, and they remain unchanged with holding potential. Only the number of events and the distribution of open states are reduced as the holding potential changes from −80 to −40 mV.

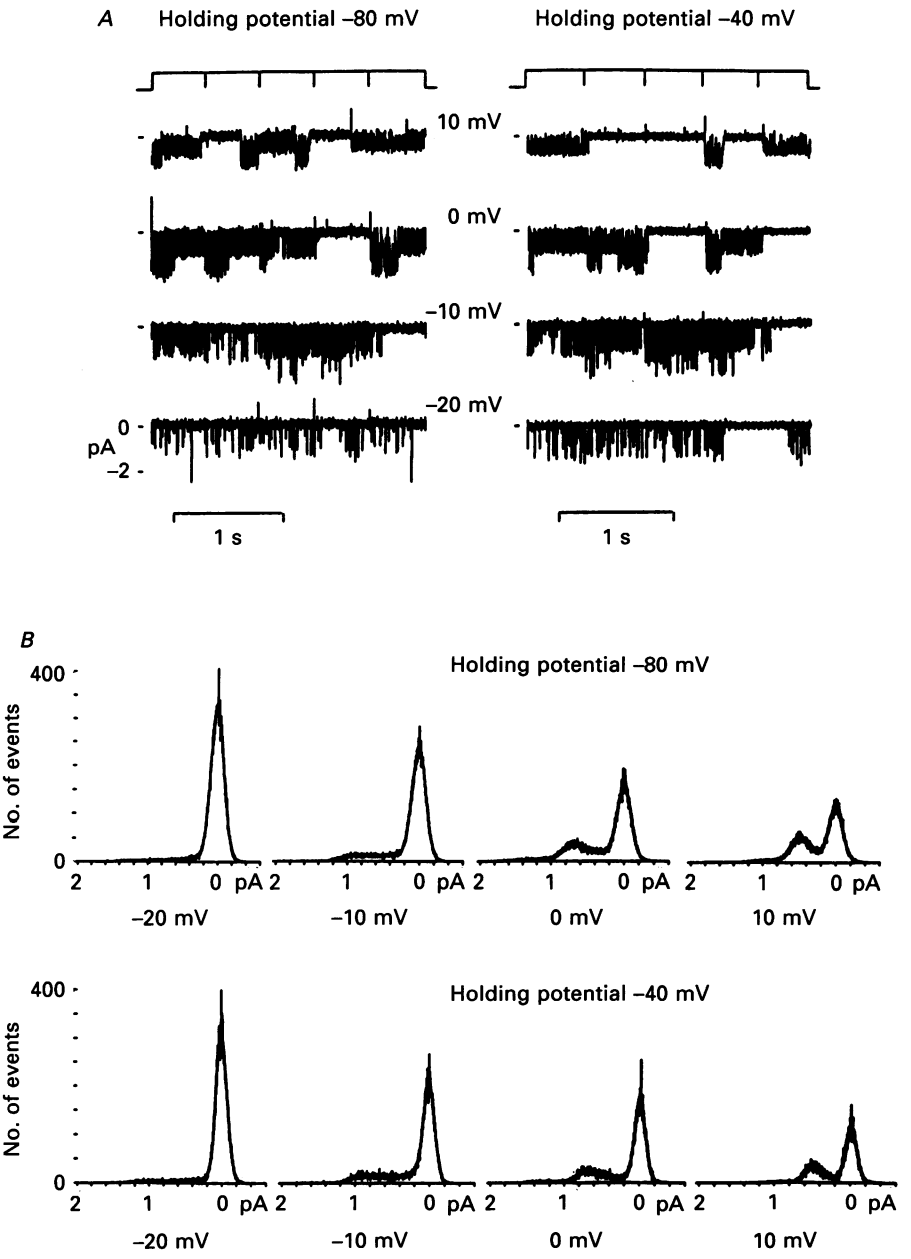

Fig. 4. *A*, examples of currents from a patch that contains two channels. In each trace we concatenated five responses to the indicated potentials. The pulses were actually separated by 1 s. The holding potential was either −80 or −40 mV. The decline in current during each test potential, which is evident in the −80 mV holding potential traces Fig. 3, is absent when there are fewer channels in the patch. Holding potential has little effect on kinetics. *B*, amplitude histograms of the current traces are virtually the same whether the holding potential is −80 or −40 mV.

These data are further analysed in the amplitude histograms of Fig. 4*B*. At test potentials of −20 to 10 mV, the relative probabilities of the open and closed states, and the amplitudes of the currents indicated by the location of the peaks, show great similarity in either holding potential.

Figure 5 summarizes these data by comparing the average currents calculated from the experiments illustrated in Figs 3 and 4. Each trace is the mean of fifteen sweeps, and at each potential we superimposed the currents obtained from −80 and −40 mV holding potentials. In Fig. 5*A* (at least five channels in the patch), the holding potential makes a dramatic difference to the average current. From −80 mV the current has an initial peak that shows a marked decline during the 500 ms test potentials. From −40 mV the current is not only smaller, but the rate of decline is less. Moreover, an appreciable tail current exists when we return the myocyte to −80 mV but not to −40 mV. In Fig. 5*B* (two channels in the patch), we see that the holding potential makes little difference to the average kinetics; however, the currents from −80 mV are slightly larger in the initial phase of the response. Although the qualitative behaviour is quite consistent, we found that individual patches have quantitative differences. (This issue is addressed more fully in Fig. 7.) Notwithstanding these patch-to-patch variations, the data represented in Fig. 5 are illustrative of a general phenomenon: in fourteen separate experiments with one to three channels in the patch, the average current was nearly unchanged by the holding potential, whereas in five separate experiments with seven to eight channels in the patch, the average currents were not only larger, as would be expected, but the decline of the current was more pronounced.

Figure 6 illustrates that the kinetics of the channel are essentially the same whether the patch is cell attached or inside out. In these experiments the bath solution was an intracellular-like medium except that it was free of all phosphorylating enzymes and substrates (see Methods). Since the bath solution contained high K^+, the cell membrane potential in these experiments was approximately zero. The indicated voltages are the absolute patch membrane potentials for both the cell-attached and the inside-out patches. The figure shows two selected traces for both configurations; in all cases these are typical observations except for the records at −10 mV, where we chose traces that contained exceptionally long openings. The long openings appear spontaneously, but they are extremely rare. Figure 7 analyses these data further. Figure 7*A* compares the open-time distributions from the same patch, which was first attached to the cell and then removed. In both cases the membrane potential step is from −80 to −10 mV. We fitted each histogram to two exponentials (see Fig. 7 legend for details). Occasionally there was on overall decrease in the number of events per unit time in the inside-out patches, but even in such cases, the shapes of the histograms are practically the same as in cell-attached patches. The faster of the two time constants depends on the filter setting, which in these experiments was 1000 Hz. Although the fast time constant contains information about channel gating, e.g. the rapid flickering process, we have not analysed it in detail. Instead we used the slower time constant, τ, as an index to compare cell-attached patches to inside-out patches. Figure 7*B* summarizes the results from four separate experiments. In both the cell-attached and the inside-out patches, τ increases monotonically as the membrane is depolarized. Unusually long

openings do occur at potentials near −10 mV (see Fig. 6), but these appear too infrequently to affect the histograms. Figure 7 shows a large variation from experiment to experiment; however, for a given patch there is no essential difference in the open-time distributions after we removed the patch from the cell and placed it in a solution free of phosphorylating enzymes or substrates.

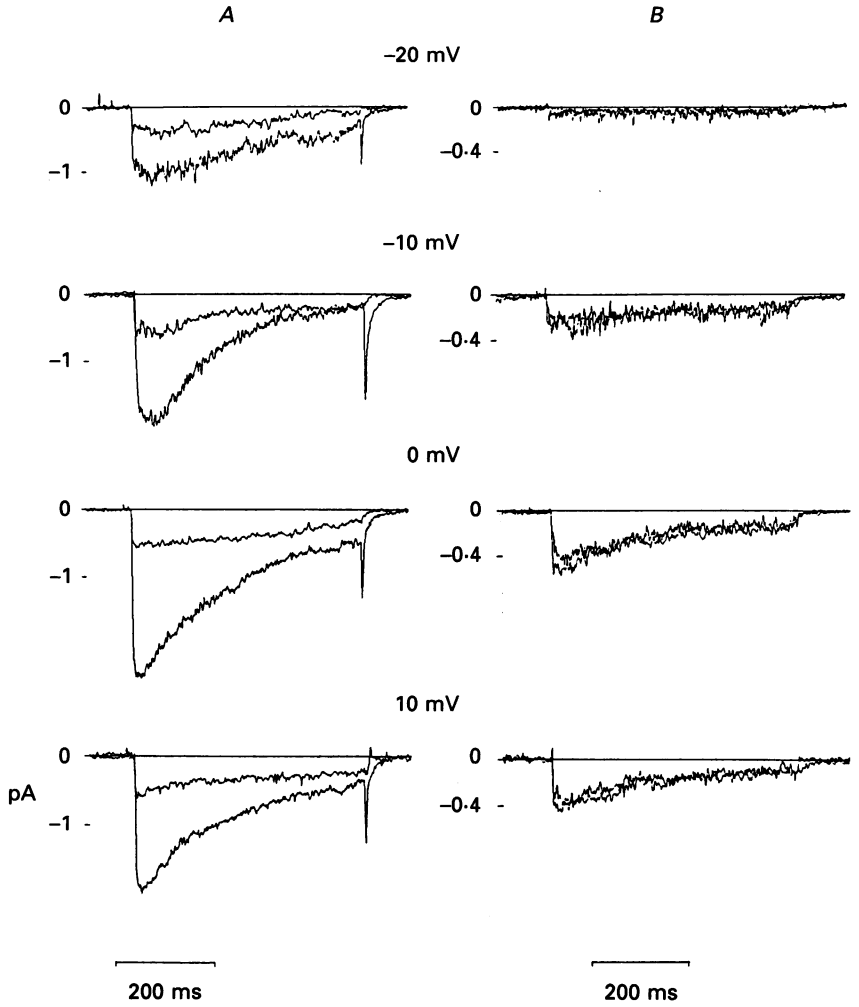

Fig. 5. *A*, the ensemble average ($n = 15$) of currents from a patch containing at least five channels (data from the experiment illustrated in Fig. 3). The larger currents are from a holding potential of −80 mV; the smaller currents are from a holding potential of −40 mV. *B*, the ensemble average ($n = 15$) of currents from a patch containing two channels (data from the experiment illustrated in Fig. 4). The traces are virtually identical whether the holding potential is −80 or −40 mV; the slightly larger currents are from a holding potential of −80 mV.

We now compare the currents from different cells with disparate current amplitudes (Fig. 8), and we compare currents from the same cell during recovery from inactivation (Fig. 9). The whole-cell experiments were done with the 20 mM-Ba^{2+} solution in the bathing medium. The preparation in Fig. 8*A* consisted of two

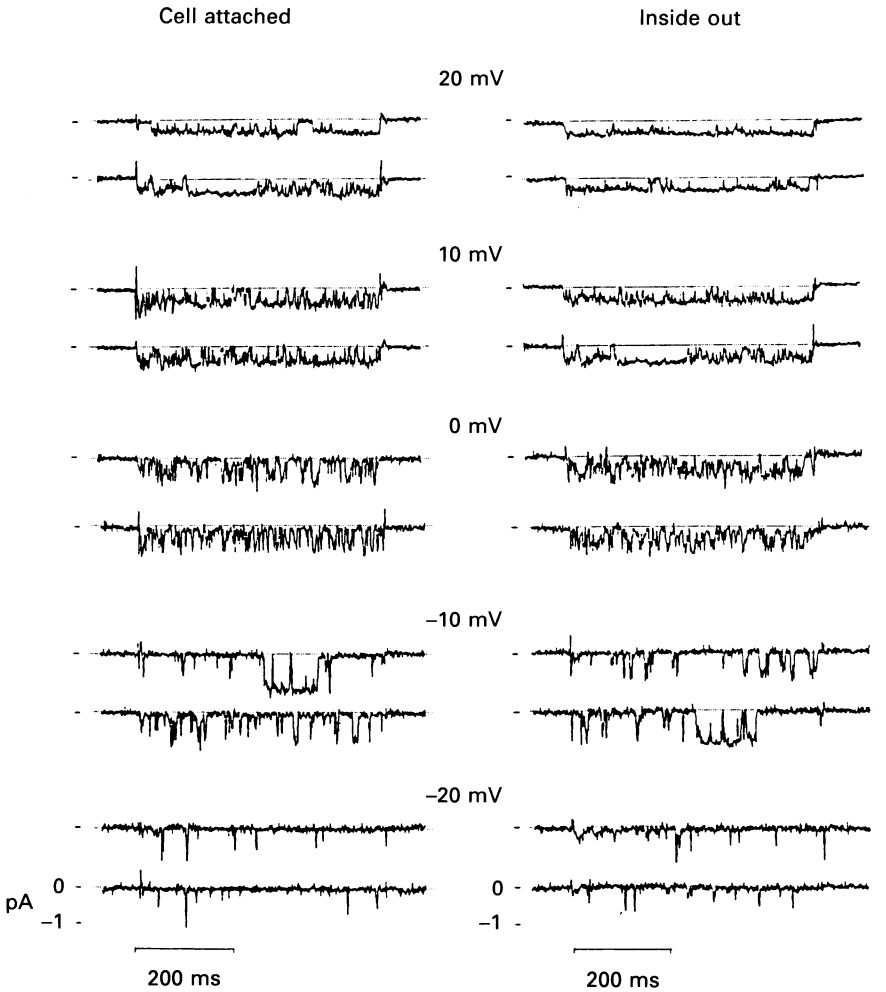

Fig. 6. Single-channel records from a cell-attached patch (left) compared to the same patch ripped off the cell and placed in an inside-out configuration (right). In these experiments the bath solution before and after the patch is ripped off the cell is an intracellular-like solution that we routinely use in whole-cell experiments (see Methods). In both panels the indicated voltages are the absolute test potentials across the patch membrane. The patch contained only one channel, and the holding potential was −80 mV. Note the qualitative similarity between the two sets of data.

or three small cells fused together. The same results were also obtained in single cells, whose diameters ranged from 8 to 16 μm. Indeed, it is difficult to distinguish, visually or electrically, several well-coupled small cells from one larger-than-average single

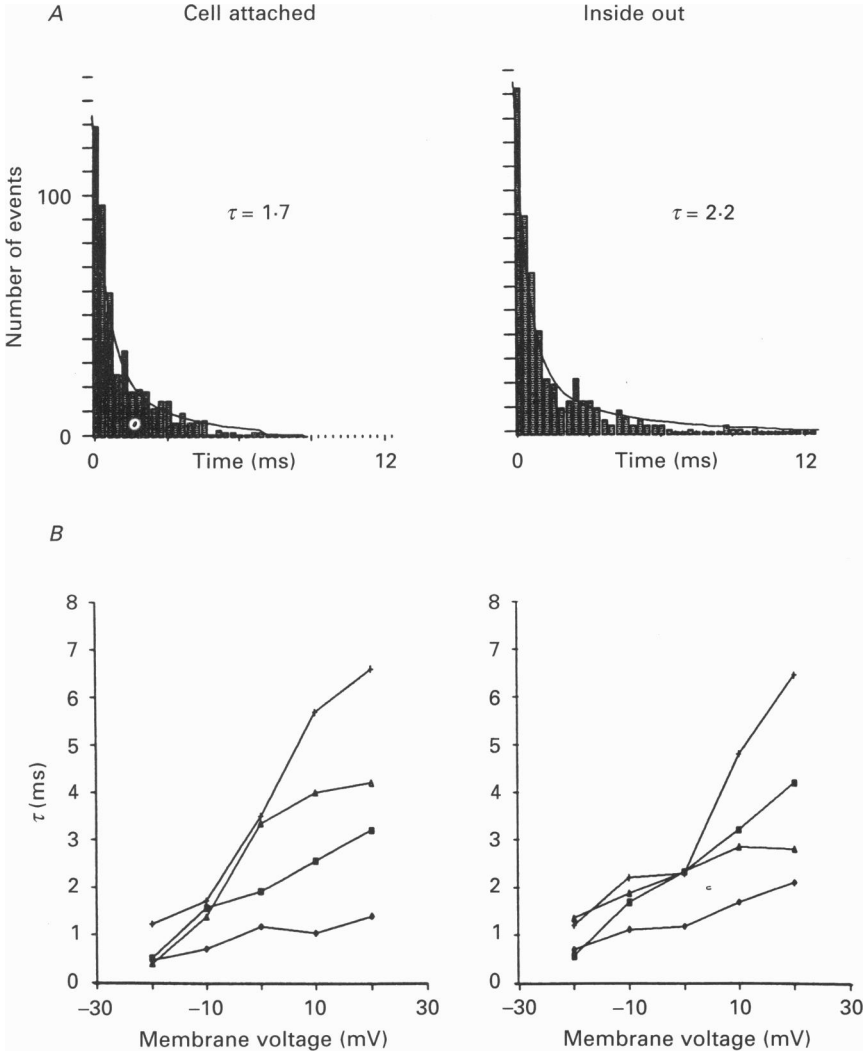

Fig. 7. Open-time histogram analysis of experiments like the one illustrated in Fig. 6, before and after rip-off (one channel per patch, holding potential = −80 mV). We fitted each histogram to two exponentials using a Marquardt's non-linear, least-squares, regressive curve-fitting routine to calculate the values of a_o, τ_o, a, and τ, in the equation $a_o[\exp(-t/\tau_o]+a[\exp(-t/\tau)]$ that most closely fit the data. An example taken from data at −10 mV is given in the top panel. For these experiments, $a_o = 698$ events, $\tau_o =$ 0·36 ms, $a = 44$ events, and $\tau = 1{\cdot}7$ ms (cell-attached), and in the same units $a_o = 805$, τ_o = 0·37, $a = 32$, and $\tau = 2{\cdot}2$ ms (inside-out). Figure 7*B* summarizes data from four experiments like the one in Fig. 6. We plot τ at various test potentials before and after ripping off the patch. There is considerable patch-to-patch variation, but within the same experiment (same symbols), τ is practically identical whether the patch is attached to the cell or exposed to an intracellular-like solution free of phosphorylating enzymes or substrates.

cell. The preparation in Fig. 8*A* had approximately four times the surface membrane area of the preparation in Fig. 8*B*. The estimates of relative size are from capacitance neutralization measurements made during the whole-cell protocol, which gave values of 10 and 2·5 pF, respectively. The peak current in Fig. 8*A* is about seven times the

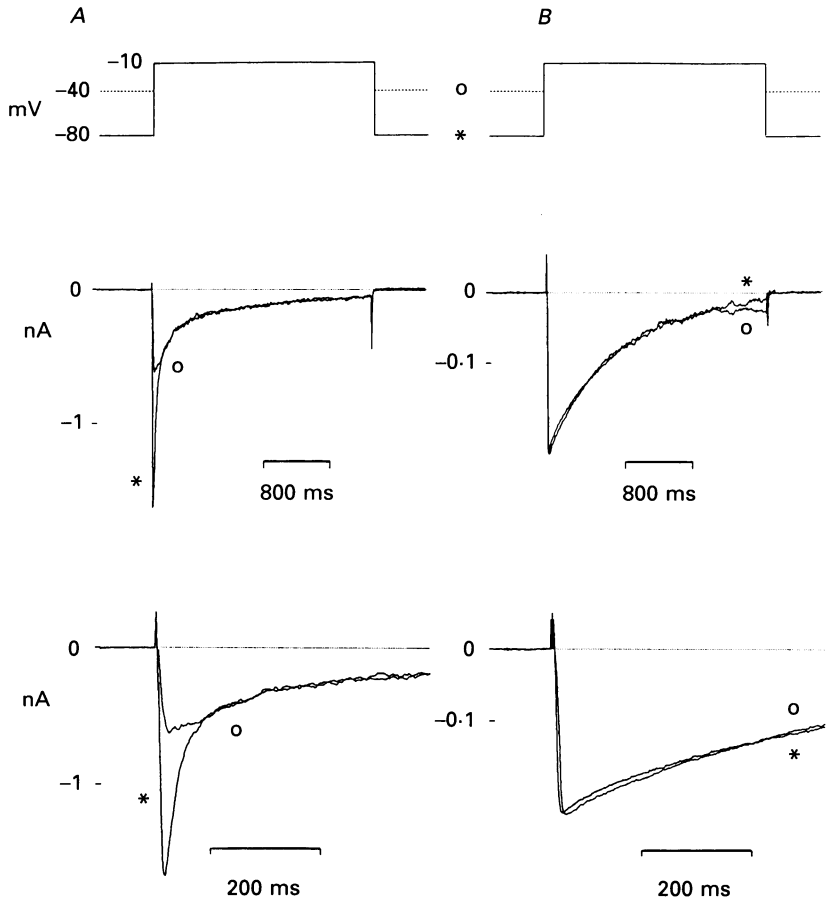

Fig. 8. Whole-cell experiments in 20 mM-Ba^{2+}. *A*, the whole-cell records from a cell preparation (see Results) with a relatively large current (0·17 pA/pF at the peak) compared to the usual current density in 7-day-old chick ventricle. The top frame shows the pulse protocol. Below are the two currents elicited from each step on a slow and fast time scale. The initial peak current with the rapid inactivation, which is indicated by the asterisk, is from a holding potential of −80 mV. The other current trace in *A*, which is missing the rapidly declining peak, is from the holding potential of −40 mV. *B*, the whole-cell records from a cell preparation (see Results) with a more typical current density for 7-day-old chick ventricle (0·09 pA/pF at the peak). The traces are virtually identical whether the holding potential is −80 or −40 mV.

peak current in *B*. Therefore, the larger current not only reflects increased surface area, but also larger current density. The figure illustrates our general finding that holding the potential at −80 or −40 mV has a pronounced result on cells with large

currents but practically no effect on cells with small currents. Solutions containing 20 mM-Ba^{2+} are generally toxic to cells from 7-day-old chick ventricle, and for that reason it was difficult to perform many experiments of the type shown in Fig. 8. We obtained records qualitatively similar to Fig. 8*A* in three experiments, two of which

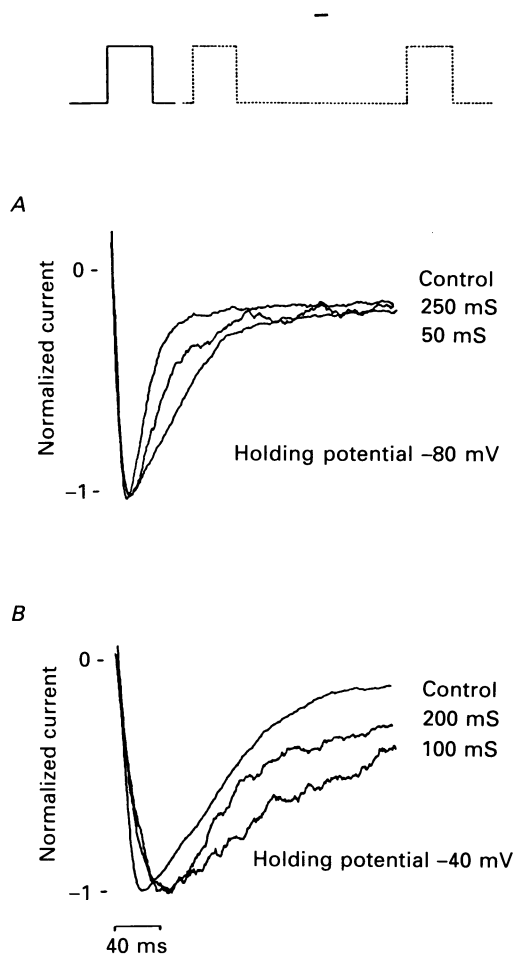

Fig. 9. Whole-cell experiments in 20 mM-Ba^{2+}. In these experiments we held single-cell preparations (see Results) at either −80 or −40 mV for 4 s and then applied consecutive, 500 ms steps to −10 mV. The time between the end of the control step (i.e. the first step) and the beginning of the second or third step appears near the current response. To facilitate comparison of kinetics, each response was normalized to the same amplitude.

were on single cells, 10–13 μm in diameter, and to Fig. 8*B* in ten experiments, six of which were on single cells, 10–13 μm in diameter.

Figure 9 shows experiments on 10–13 μm-diameter single cells during their recovery from inactivation. In *A* we held the cell at −80 mV for 4 s, stepped it to −10 mV for 500 ms, and then repeated the step at different intervals. These subsequent steps resulted in smaller currents; however, to facilitate comparison, we

normalized the currents to the same peak amplitude. The control current at peak value was 890 pA; after a 50 ms delay (measured from the end of the control step), the current was 380 pA; after a 250 ms delay, the current was 855 pA. The current fully recovered its amplitude and rate of inactivation after 0·6 s. Figure 9*B* repeats

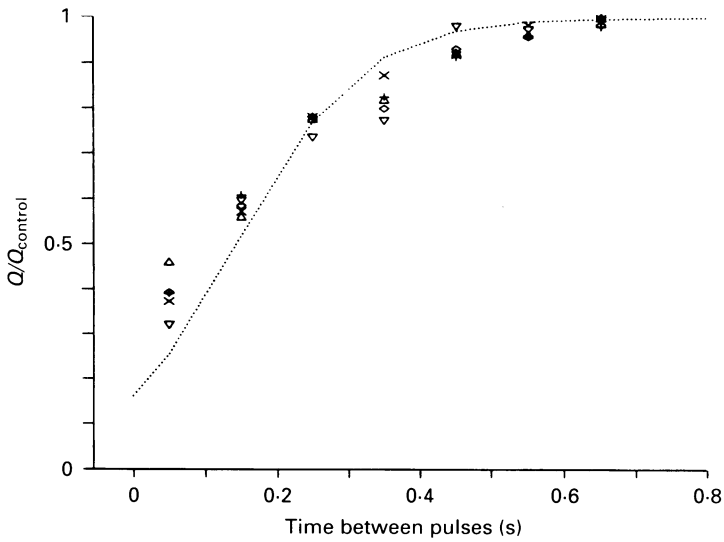

Fig. 10. The recovery curve of five whole-cell experiments like the one in Fig. 9*A*. The vertical axis is the normalized integral (500 ms) of the response. The horizontal axis is the time between the end of the control step and the beginning of the second, third, etc. step. The dotted line is theoretical (see Results).

this experiment on another single cell, with the holding potential at −40 mV. The peak amplitudes in this case were 574 pA (control), 150 pA (100 ms delay), 198 pA (200 ms delay). Because cells rapidly deteriorate in 20 mM-Ba^{2+} solutions, we used separate cells for the experiments illustrated in *A* and *B*, and we required full return to control levels after a 4 s interval. We obtained records qualitatively similar to those in Fig. 9*A* in five experiments (three on single cells 10–13 μm in diameter), and to *B* in six experiments (three on single cells 10–13 μm in diameter).

Figure 10 shows the complete recovery curve for five experiments with conditions as in Fig. 9*A*. The area under the response is plotted as a function of time (from the end of the control step to the beginning of the test step; steps 500 ms in duration). To compare experiments, the data are normalized to the control. Complete recovery occurs in about 600 ms. The dotted line through the data was generated by simulating the recovery experiment with the model illustrated in Fig. 11. Using the approximate conditions of Fig. 9*A*, we challenged the model at seven consecutive intervals and calculated the integrals of the responses. The dotted line was produced by connecting these theoretical points.

Figures 5, 8, and 9 show that whether the number of channels in the membrane is inherently lower, or whether the number of channels is effectively reduced by voltage or by incomplete recovery, smaller currents have slower inactivation. Figure 11

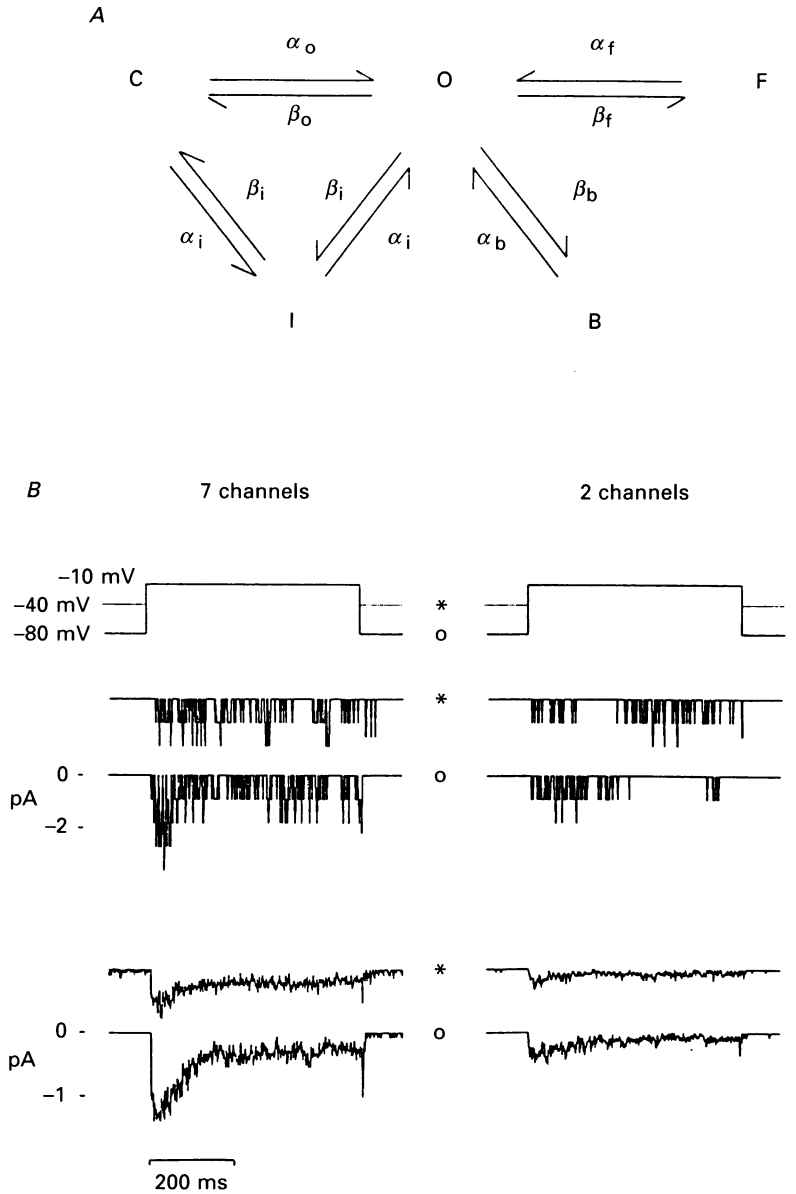

Fig. 11. Model of L-type Ca^{2+} channels carrying 20 mM-Ba^{2+}. *A* shows the state diagram; it contains one open state O, a closed state C, an inactive state I, a flicker state F, and a blocked state B. The arrows indicate the allowed transitions. All αs and βs are voltage-dependent rate constants except β_b, which depends on the current through the population of currents as described in the text. See Table 1 for the values of the rate constants. When the channel is open, the current is $i\text{–}V = \gamma(V-E)$; all other states have zero conductance. *B*, the responses of the model using seven or two channels. From top to bottom, these panels show the voltage protocol, a typical current from seven (or two) model channels, and the average current (thirty runs) from seven (or two) model channels. Contrast these theoretical results with measured currents at −10 mV in Figs 3, 4, and 5.

outlines a model that accounts for the main features of these experiments. The model channel has five states and seven different rate constants. Four of the rate constants, α_o, β_o, α_i, and β_i, are the conventional voltage-dependent parameters of activation and inactivation analogous to those in standard models of cardiac excitability (Beeler & Reuter, 1977). The rate constants $\alpha_f = \beta_f$ allow the open state to flicker.

TABLE 1. Values of constants in the rate equations

$\xi \exp a(V-b)/[1+\exp a(V-b)]$

	a(mV)$^{-1}$	b(mV)	ξ(ms)$^{-1}$
α_o	0·20	−15	0·2
β_o	−0·05	−40	2·0
α_i	−0·05	−60	0·005
β_i	0·20	−50	0·005
$\alpha_f = \beta_f$	−0·10	−10	1·0
α_b	−0·06	−80	1·0
β_b	$\theta = 1$ s	$k = 1$ nC ms^{-1}	

$i(V) = \gamma(V-E)$

$\gamma = 18$ pS, $E = 40$ mV

The parameter β_b describes the reaction rate to the blocked state. For each channel it is made proportional to the total charge $q(t)$ that collects on a leaky integrator from the current $I(t) = ni(t)$ through n channels. The charge collected on the integrator is:

$$q(t) = \exp(-t/\theta)\,[q_o + \int_\theta^t \exp(u/\theta)\, I(u)\, du],$$

where θ is the time constant of the leaky integrator, and q_0 is the initial charge. If $I(t)$ is constant over the computation step Δt, and if Δt is small compared to θ, then:

$$q_0 \approx I_0 \Delta t_0,$$

$$q_1(\Delta t_0 + \Delta t_1) \approx q_0 + I_1 \Delta t_1 - q_0 \Delta t_0/\theta, \text{ etc.}$$

We use this formula for the iteration procedure (I in μA, t in ms and $\Delta t = 0{\cdot}3$ ms) and let:

$$\beta_b = kq(t),$$

where k is a constant that converts nC to ms^{-1}. At any time t, after the onset of the simulation, the rate of conversion for each channel to state B gains in proportion to the number of ions passing through n channels and loses in proportion to the number that leak away with time constant v. The rate constant α_b describes the unblocking reaction and is simply voltage dependent.

All voltage-dependent rate constants are described by the equation:

$$\text{rate} = \xi \exp a(V-b)/[1+\exp a(V-b)].$$

Values of ξ, a, and b for the voltage-dependent rates, and values of θ and k for the current-dependent rate, appear in Table 1. For the open-channel i–V relationship, we used the nominal values of 10 pS for conductance and 40 mV for the reversal potential (Fig. 2). Figure 11B shows representative responses from seven channels

held at −40 or −80 mV stepped to a test potential of −10 mV. Underneath these are the average of thirty such responses for each holding potential. On the right-hand side we repeated the simulation for two channels.

Figure 12 compares the theoretical response of 10, 100, and 1000 channels to the same stimulus, −80 to −10 mV (*A*), and the response of 100 channels to two different

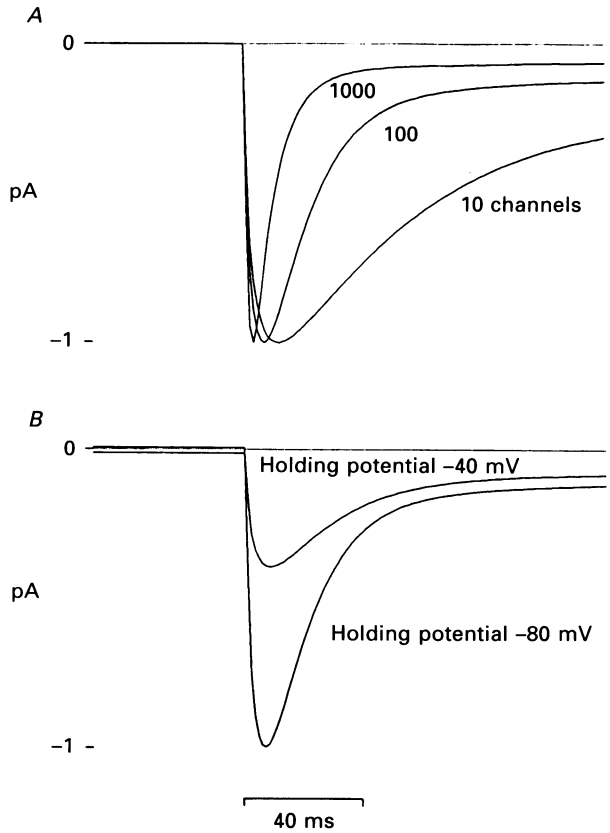

Fig. 12. Model of L-type Ca^{2+} channels carrying 20 mM-Ba^{2+}. Unlike Fig. 11, these calculations were done in the macro-mode of MACROCHAN, resulting in ideally smoothed current traces (DeFelice, Goolsby & Huang, 1985). *A*, the stimulus is −80 mV holding potential and −10 mV test potential. We varied only the number of channels in the model, leaving all other parameters in the model the same (Table 1). The current amplitudes increase with channel number, but to compare kinetics we normalized all current peaks to the same arbitrary value. *B*, the number of channels (100) and the test potential (−10 mV) are constant, but the holding potential is either −80 or −10 mV. In this case the two currents are on the same scale, so that the decrease in the peak current from −40 mV reflects the actual change in current. Contrast these theoretical results with Figs 8 and 9.

stimuli, −80 to −10 and −40 to −10 mV (*B*). We assume each channel responds to the total current in the ensemble, and each response initiates from steady-state conditions at the holding potential. In *A* we show the initial phases normalized to the same peak value. It is evident from this calculation that as the number of channels

increases, the closing kinetics become faster. In *B*, we compare 100 channels on the same amplitude scale. This simulation shows that as the number of active channels is decreased by holding at −40 mV, the initial peak is attenuated and the closing kinetics are slower. Though not explicitly shown, it is evident that in such simulations, challenging the channels prior to their full recovery from inactivation would decrease their effective number, reduce the total current, and slow the kinetics. Thus Fig. 12 demonstrates that rapid kinetics measured in whole-cell experiments, such as those shown in Fig. 8*A*, may be generated by a model in which L-type Ca^{2+} channels having voltage-dependent inactivation and current-dependent block. The model also explains how more negative holding potentials (Fig. 8*A*), fewer channels per unit area (Fig. 8*B*), or stimulation before recovery from inactivation (Fig. 8) – in short, any condition that reduces the current – slows L-type channel kinetics.

DISCUSSION

Ca^{2+} current is self-limiting only if channel density is sufficiently high

Although the mechanisms are unknown, evidence mounts to support the hypothesis that the passage of Ca^{2+} ions through L-type Ca^{2+} channels is somehow self-limiting. Lux & Brown (1984) reasoned that if this were indeed the case, there ought to be direct consequences on Ca^{2+} channel kinetics at the level of single pores. Finding no correlation between the Ca^{2+} current during individual openings and the time spent in the subsequent closed state, these authors concluded that Ca^{2+} ions produce no inactivation of the Ca^{2+} channel. A similar expectation, that unitary Ca^{2+} channel currents should drop during long openings, is never observed. Experiments performed by Lux & Brown (1984) were carried out in 40 mM-Ca^{2+} in cell-attached patches on neuronal cell bodies of *Helix*. Single-channel kinetics were independent of the holding potential. Whole-cell currents had virtually the same shape as the average of the unitary events, and similar results were obtained in both single-channel and whole-cell experiments upon substituting Ba^{2+} for Ca^{2+}. These data are strikingly similar to our cell-attached results with one or two channels in the patch, and to our whole-cell experiments at low ($< 0{\cdot}1$ pA pF^{-1}) current densities. The patches in the experiments of Lux & Brown (1984) also contained only one or two channels. How can we account for the absence of Ca^{2+}-induced inactivation in individual channel records in the face of clear contradictory evidence in macroscopic experiments (Kass & Sanguinetti, 1984; Lee *et al.* 1985)? Yue *et al.* (1991) showed that in 160 mM-Ca^{2+} the current through an individual channel can effect its own gating. However, their experiments do not explain the contradiction between single-channel and whole-cell data at lower concentrations of the conducting ion. A possible explanation that may apply to more physiological conditions is the following: whereas the current through one channel may be unable to establish the concentration necessary to block the pore, the current through groups of channels sufficiently close to one another can provide this condition.

Is the limiting mechanism a separate blocked state?

Does the Ca^{2+}-mediated decline in current work by increasing the decay to the voltage-gated inactivate state or by populating a separate blocked state? Little doubt remains that voltage-gated inactivation exists (Campbell *et al.* 1988*a*;

Rosenburg, Hess & Tsien, 1988). Rosenberg *et al.* found a voltage-dependent component in reconstitution experiments in lipid bilayers. They showed that millimolar concentrations of Ca^{2+} ions on the internal face of the membrane decrease Ba^{2+} currents but not the rate of inactivation, and that internal Ca^{2+} concentrations up to 10 mM reduce the Ba^{2+} conductance considerably but not channel kinetics. In these bilayer experiments, as in cell-attached patches (Cavalie *et al.* 1986), the rate of inactivation varies considerably from channel to channel. Rosenburg *et al.* (1988) rule out models of Ca^{2+}-mediated inactivation in which Ca^{2+} interacts with high-affinity binding sites; however, they do not eliminate models with low-affinity sites or mechanisms that rely on indirect actions of Ca^{2+} that may have been lost in the bilayer experiments. Lansman, Hess & Tsien (1986) show that, in guinea-pig ventricle, increasing the concentration of Mg^{2+} ions from 0 to 5 mM in cell-attached patches progressively increases the number of rapid closures of the Bay K 8644-induced, long openings of Ca^{2+} channels conducting 50 mM-Ba^{2+}. A similar effect of Mg^{2+} ions on Ca^{2+} channels was obtained in frog atrial myocytes by Campbell *et al.* (1988*a*). Mg^{2+} reduces Ba^{2+} current by an increase in flickering, but Ca^{2+} reduces it by a reduction in channel conductance. In addition, Mg^{2+} block is greater at negative potentials, but Ca^{2+} block is voltage independent. These experiments support the idea that Ca^{2+} can leave the pore rapidly when the pore is occupied by divalent ions, and that the Ca^{2+} channel is a pore in which blocking ions compete with permeable ions for several binding sites (Hess & Tsien, 1984). The extent to which Ca^{2+} block of Ba^{2+} currents applies to Ca^{2+} block of Ca^{2+} currents is unclear. What remains certain is that voltage-gated inactivation occurs, but no absolute experimental distinction between blocking, reduced permeability, and inactivation prevails.

The model we chose demonstrates that the explicit assumption of a blocked state can explain the dramatic difference between the kinetics of one channel and the kinetics of many channels if they are close enough to interact via the net Ca^{2+} current that passes through them. It also describes the wide variety of kinetics that have been observed for L-type currents in whole-cell experiments. These kinetics range from relatively slow 'inactivation' phases to much more rapid declining phases, a variability that we now suggest is a consequence of the (perhaps non-uniform) proximity of Ca^{2+} channels in the membrane. Another feature of patch experiments that the model predicts is the size and the time course of tail currents. Note that in Fig. 1 the tail currents are excluded from the display and from the histogram analysis; however, they are included in the ensemble averages shown in Fig. 5. Although we have not analysed tails in detail, generally the differences in tail currents generated from the two holding potentials are too large and the decay times are too slow to be explained by driving force alone. Unusually slow tail currents have also been observed in other preparations (Campbell *et al.* 1988*a*; Campbell, Robinson & Shibata, 1988*b*; Bean & Rios, 1989). Significant in this regard is the rate constant α_b, which returns the channel to the open state (Fig. 11). In our model it is a steep function of voltage that clears the channel of the blocking ions more effectively at -80 than at -40 mV. The model therefore offers an explanation of tail currents that is different from the electrogenic Na^+–Ca^{2+} exchanger mechanism proposed by Campbell *et al.* (1988*b*).

The model

The model does not attempt to describe the data in all detail. Indeed, the variability from experiment to experiment, reported by many authors, e.g. Cavalie, Pelzer & Trautwein, (1986), and the complexity of kinetics, e.g. the existence of modes recently affirmed by Pietrobon & Hess (1990), make a comprehensive description of L-type Ca^{2+} channels unlikely with the rudimentary scheme in Fig. 11. In the diagram the open, closed, and inactive states represent the minimum standard representation of a time-variant, voltage-dependent channel. Evidence for more closed states is reviewed in Pelzer, Pelzer & McDonald (1990). We included a flickering state to account for the brief closings; otherwise, we kept the model as simple as possible. This simplification incorporates a modified version of the standard equation for the voltage-dependent rate constants (Table 1). We use nominal values of these parameters that fit the data by inspection rather than by optimization.

We diverge from the conventional diagram by introducing a current-dependent reaction that blocks the channel. The idea behind this additional closed state is that a concentration of charge builds up after ions pass through the channel, and this accumulation blocks the current by an unknown mechanism. The ions may also diffuse into the cytoplasm, thereby reducing the blockage. Evidently the inherent buffering and release mechanisms in the cell, as well as restricted spaces near the inner membrane surface, play a role in this build-up and dispersal of ions (Fischmeister & Horackova, 1983; Lederer, Niggli & Hadley, 1990). However, the natural sequestering mechanisms are for Ca^{2+} ions, and too little is known about Ba^{2+} to model diffusion or buffering in any detail. For this reason we merely assume the blocking ions leak away by some mechanism with a single time constant. The build-up and dispersal are modelled by leaky integrator, the rate to the blocked state being proportional to the accumulation of ions. (The electrical equivalent of a leaky integrator is a resistor and capacitor in parallel; however, we imply no explicit mechanism by evoking the equation for a leaky integrator, only the general notion of build-up and simultaneous decay.) If a channel is open the chance it will be blocked increases with each ion that passes through, but after one time constant each ion is only 1/e as likely to block. Only the probabilities of changing states are altered; thus, the open channel current is constant. From Table 1 the value of θ that fits the data is 1 s. This time could reflect not only passive diffusion away from the channel, but also Ba^{2+} uptake and release mechanisms within the cell, and ought to change with temperature. The choice of room temperature was dictated by convenience, and because lower temperatures slow kinetics and increase temporal resolution. At present we interpret θ only as the typical interval necessary for Ba^{2+} ions, at room temperature, to leave their domain of influence near the inner channel mouth.

Modes

How does such a model fit with the idea of mode kinetics? In cardiac cells L-type Ca^{2+} channels carrying Ba^{2+} may demonstrate three kinds of kinetics: brief openings with low probability (referred to as mode 1), long openings interrupted by brief closings (mode 2), and no openings (null mode, see Hess *et al.* 1984). Under this nomenclature, dihydropyridines like Bay K 8644 and β-adrenergic agonists like

isoprenaline enhance the Ba^{2+} current by promoting mode 2 kinetics. Long-lasting openings may occur in the absence of agonists (Hess *et al.* 1984), a result that suggests they are intrinsic to the channel. Antagonists like nifedipine suppress the current by favouring the null mode. As demonstrated in Fig. 1, we may increase the probability of channels being in the open state by merely depolarizing the membrane (Mazzanti & DeFelice, 1990*b*; Pietrobon & Hess, 1990). This steady-state, voltage-activated increase in open channel probability is distinct from the long openings that occasionally occur at a voltage when the open times are normally much briefer. We selected samples of these rare events in Fig. 6, at −10 mV. We also find them at −20 mV (not shown), but in general they are extremely infrequent. Similar openings occur in beating heart cells (Mazzanti & DeFelice, 1990*b*). The model we propose here does not account for these unusual currents, and it therefore provides no evidence for representations that flip between kinetic schemes (Hess *et al.* 1984; Pietrobon & Hess, 1990; Yue, Herzig & Marban, 1990; Yue & Marban, 1990) as opposed to those with continuous kinetics interpreted within one kinetic scheme (Brown, Kunze & Yatani, 1984; Cavalie *et al.* 1986; Lacerda & Brown, 1989). Our focus is therefore not on the existence of modes, to which some of our data point, but on the interplay between voltage gating, current modulation, and the density of pores.

Phosphorylation

Does the voltage-dependent gating of L-type Ca^{2+} channels require the Ca^{2+} channel to be phosphorylated? It has been known for some time that Ca^{2+} channels are modulated *in vivo* by cyclic AMP-dependent phosphorylation (Tsien, Giles & Greengard, 1972; Osterrieder, Brum, Hescheler, Trautwein, Flockerzi & Hofmann, 1982; Reuter, 1983; Bean, Nowycky & Tsien, 1984; Lacerda, Rampe & Brown, 1988). Numerous studies attribute Ca^{2+}-channel run-down in cell-detached patches to cyclic AMP-dependent phosphorylation, and Armstrong & Eckert (1987) take this argument a step further in GH3 cells by implicating a catalytic subunit of cyclic AMP-dependent protein kinase on the cytoplasmic side of the patch. Using inside-out patches, Armstrong & Eckert showed that when they added the catalytic subunits plus ATP to the cytoplasmic side this restored L-type Ca^{2+} channel activity to patches that had lacked activity for several minutes. A possible explanation of experiments in which little run-down occurs is that ripped-off patches contain a membrane-bound kinase, and the bathing solutions contain ATP.

We may evoke such an explanation for cell-detached patch experiments, although our solutions contain neither the enzyme nor the phosphorylating substrate. If voltage-dependent gating depends on the phosphorylation of sites on L-type Ca^{2+} channels, our experiments indicate that the state of phosphorylation is unaltered when the patch is removed from the cell (Fig. 6). One possible explanation for the range of kinetics from patch to patch (Fig. 7) might be variance in the degree of phosphorylation. If this were the case, Ca^{2+} currents would include not only the average of statistically identical elements but also the average over unequal phosphorylation states with qualitatively similar but quantitatively distinct kinetics.

Ba^{2+} versus Ca^{2+} currents

To what extent will our conclusions apply to the natural charge carrier? Bean (1985) showed, through the differential voltage dependence and pharmacology, that two kinds of Ca^{2+} channels exist in atrial cells (I_{fast} and I_{slow}, also called T-type and L-type currents). This separation was demonstrated in both 115 mM-Ba^{2+} and in 5 mM-Ca^{2+} in whole-cell experiments. From Bean's results (1985, see Figs 2 and 4), we see a clear acceleration of channel kinetics in Ca^{2+} over Ba^{2+} for the L-type component. In 20 mM-Ca^{2+} *versus* 20 mM-Ba^{2+}, the amplitude is roughly five times less and the Ca^{2+} currents are again faster and have a more rapidly declining, or steeper inactivation phase. Moreover, in 10 mM-Ba^{2+} in ventricular cells where only L-type Ca^{2+} channels exist (Bean & Rios, 1989), the kinetics appear to be somewhat slower than they were in the 20 mM-Ba^{2+} solutions of the earlier study (Bean, 1985). In spite of the different conditions of the two experiments, this comparison indicates that the declining phase of Ba^{2+} currents depends on Ba^{2+} concentration. McDonald *et al.* (1986), studying the voltage-dependent properties of macroscopic and elementary Ca^{2+} channel currents in guinea-pig ventricular myocytes, found that their results corresponded to the ion permeation model of Hess & Tsien (1984). At low levels of Ca^{2+} and Ba^{2+} the properties of L-type channels are approximately equal; however, McDonald *et al.* (1986, see Fig. 1) demonstrates an obvious slowing of the kinetics as 3·6 mM-Ba^{2+} replaces 3·6 mM-Ca^{2+}. Hirano *et al.* (1989) performed similar comparative studies in Purkinje cells. Replacing 5 mM-Ca^{2+} by 5 mM-Ba^{2+} increases the amplitude of the L-component and markedly slows its kinetics. Ba^{2+} replacement has practically no effect on the conductance or kinetics of T-type currents at these low concentrations. These experiments indicate that we may expect the results obtained with Ba^{2+} to apply to the natural condition with Ca^{2+}, but only to a limited degree. The two conditions may converge as the ionic concentration decreases, but we expect that the inactivation kinetics of Ca^{2+}-conducting channels will always be faster.

L-type currents

Though some cardiac cells have both T-type and L-type Ca^{2+} channels, particularly atrial cells (Bean, 1985) and Purkinje cells (Hirano *et al.* 1989), there is little doubt that the currents we see are from a single category of L-type currents. The cells used in this study, when measured in physiological solutions containing 1·5 mM-Ca^{2+}, have inward Ca^{2+} currents that are blocked completely by nifedipine. We can increase the amplitudes of these same currents by adding isoprenaline to the bath or by adding cyclic AMP and ATP to the whole-cell electrode. In our experimental solution, which contained 20 mM-Ba^{2+}, both the initial and the late components of the single-channel currents have conductances that are L-type (18 pS, Yue & Marban, 1990), and the analogous components of the whole-cell Ba^{2+} currents are completely blocked by 20 μM-nifedipine.

Depending on current density the whole-cell kinetics can be quite different, with some currents displaying a marked declining phase and a dependence on holding potential that are superficially similar to recordings obtained from preparations that contain both L-type and T-type channels (Fig. 8). Similar remarks apply to our

experiments on cell-attached patches (Fig. 5). It is possible that some of our patches contain two types of channels, one sensitive to holding potential and the other not. Patches with many channels would be more likely to have both kinds, and some of our data seem to fit the familiar classification scheme for T-type and L-type channels. Against this interpretation are the following observations: (a) all patches with only one or two channels contained the L-type, and none contain T-type, as categorized by channel conductance; (b) in patches with five or more channels, all channels have the same L-type conductance; (c) whole-cell recordings in 20 mM-Ba^{2+} show qualitatively similar behaviour to the cell-attached patches, and the kinetics and pharmacology of the Ba^{2+} currents are L-type; (d) nifedipine blocks whole-cell Ca^{2+} currents in these cells, and cyclic AMP enhances them; thus, 7-day-old chick ventricle cells have no T-type currents, though later stages may (Kawano & DeHaan, 1989). It might be possible that some of the fast current elicited from −80 mV is carried by Na^+ ions. However, we believe this is not the case because the bath solution contains 0·01 mM-TTX, and because there are no TTX-resistant Na^+ currents in this preparation (Mazzanti & DeFelice, 1987*a*, *b*; Wellis *et al.* 1990).

Channel density

We note for comparison that in guinea-pig ventricle, in which current density is high (25 pA pF^{-1}, McDonald *et al.* 1986), the L-type current shows a rather steep initial decline (−50 to −10 mV step in 3·6 mM-Ca^{2+}). In contrast, L-type currents in canine atrium, in which current density is lower (about 0·5 pA pF^{-1}, Bean 1985), show no similar steep decline in initial current (−30 to −10 mV step in 5 mM-Ca^{2+}); rather, this L-type current inactivates slowly over hundreds of milliseconds. Given the different tissues and unequal conditions of the two experiments, this comparison may be somewhat artificial. A stronger comparison is provided by a recent study carried out under constant conditions in cells that express variable current densities at different stages of development. Investigating L-type channels in newborn and adult rabbit ventricle cells, Osaka & Joyner (1991) showed that as the current density doubles, from about 5 to 10 pA pF^{-1} at +10 mV test potentials in 1·8 mM-Ca^{2+}, the inactivation phase of this current becomes measurably faster. The average half-time of inactivation $T_{1/2}$ was 12·8 ± 1·9 ms in newborns and 10·7 ± 1·4 ms in adults. A parallel decrease occurred in 1·8 mM-Ba^{2+}. The voltage dependence of $T_{1/2}$ and the steady-state activation and inactivation parameters were the same for the two groups, suggesting that higher density currents increase the Ca^{2+}-dependent component of inactivation. Such developmental effects are thought to be distinct from sarcoplasmic reticulum contributions. The interpretation is further supported by the overlap of data in adults and newborns with higher or lower current densities within the same tissue class.

Recovery from inactivation

Whether the number of channels is inherently low, or whether the number is, in effect, made lower by re-stimulating the cell before it has fully recovered from inactivation, the qualitative effect is the same. The experimental findings are illustrated in Figs 5, 8 and 9, and the theoretical results corresponding to these cell-attached patch and whole-cell data are in Figs 10, 11, and 12. Figure 12*A* describes

the effect on kinetics of channel reduction regardless of cause (the peaks are normalized). Figure 12*B* shows the effect of holding potential only (the relative size of the peaks are preserved). If the kinetics of L-type channels were strictly voltage-dependent, one would expect identical voltage steps to give identical currents (except for size) regardless of channel number, contrary to our experiments (Figs 9 and 10).

Conclusion

The findings of this paper are consistent with the idea that L-type Ca^{2+} channel inactivation is both voltage and current dependent. Isolated channels may not show current-dependent inactivation. Voltage-dependent and current-dependent inactivation interact, as summarized in Fig. 12. If channel density is high, the declining phase of the initial current can be extremely fast. The cumulative action of blocking ions on adjacent channels causes this steep inactivation. This hypothesis assumes neither channel clustering nor uniform distribution. Our patch data suggests that clustering does occur and that a minimal local density is essential for blocking to occur. Our whole-cell experiments do not necessarily imply clustering. Taken alone, they are also consistent with low uniform density and, in some cells, occasional clustering that may give the impression of high uniform density.

Finally, we expect that the current-dependent block and its effect on L-type Ca^{2+} channel kinetics will be stronger (at equal concentrations) for Ca^{2+} currents than for Ba^{2+} currents. Therefore our hypothesis may apply to Ca^{2+} currents in physiological conditions. At a given density the number of available Ca^{2+} channels may decrease with holding potential or during recovery from inactivation: if evoked current is diminished, the block is less effective, and the kinetics are slower. This interpretation may help explain the wide variety of kinetics that are reported by L-type currents, and the reason why single-channel data do not scale to macroscopic data.

We wish to thank Ms B.J.Duke for preparing the solutions and the tissue cultures, Mr W.N.Goolsby for the electronics and computer support necessary for this work. We particularly acknowledge Bill Goolsby's contribution to the expansion of MACROCHAN to include the current-dependent process described in the text, and also for his help in preparing Fig. 11. In addition we wish to thank Drs Isabella Gourdon, Robert L. DeHaan, and Claudia Adkison for criticizing and editing the manuscript. This work was supported by National Institutes of Health Grant HL-27385.

REFERENCES

ARGIBAY, J. A., FISCHMEISTER, R. & HARTZELL, H. C. (1988). Inactivation, reactivation and pacing dependence of calcium current in frog cardiocytes: correlation with current density. *Journal of Physiology* **401**, 201–226.

ARMSTRONG, D. & ECKERT, R. (1987). Voltage-activated Ca channels that must be phosphorylated to respond to membrane depolarization. *Proceedings of the National Academy of Sciences of the USA* **84**, 2518–2522.

BEAN, B. (1985). Two kinds of calcium channels in canine atrial cells. *Journal of General Physiology* **86**, 1–30.

BEAN, B. P., NOWYCKY, M. C. & TSIEN, R. W. (1984). β-adrenergic modulation of Ca channels in frog ventricular heart cells. *Nature* **307**, 371–375.

BEAN, B. P. & RIOS, E. (1989). Nonlinear charge movement in mammalian cardiac ventricle cells. *Journal of General Physiology* **94**, 65–93.

BEELER, G. W. & REUTER, H. (1977). Reconstruction of the action potential of ventricular myocardial fibres. *Journal of Physiology* **268**, 177–210.

BREHM, P. & ECKERT, R. (1978). Ca entry leads to inactivation of Ca current in *Paramecium*. *Science* **202**, 1203–1206.

BREHM, P., ECKERT, R. & TILLOTSON, D. (1980). Calcium-mediated inactivation of calcium current in *Paramecium*. *Journal of Physiology* **306**. 193–203.

BROWN, A. M., KUNZE, D. L. & YATANI, A. (1984). The agonist effect of dihydropyridines on Ca channels. *Nature* **311**, 570–572.

CAMPBELL, D. E., GILES, W. R. & SHIBATA, E. F. (1988*a*). Ion transfer characteristics of the calcium current in bull-frog atrial myocytes. *Journal of Physiology* **403**, 239–266.

CAMPBELL, D. I., GILES, W. R., ROBINSON, K. & SHIBATA, E. F. (1988*b*). Studies of the Sodium–Calcium exchanger in bull-frog atrial myocytes. *Journal of Physiology* **403**, 317–340.

CAVALIE, A., OCHI, R., PELZER, D. & TRAUTWEIN, W. (1983). Elementary channels through Ca channels in guinea-pig myocytes. *Pflügers Archiv* **398**, 284–297.

CAVALIE, A., PELZER, D. & TRAUTWEIN, W. (1986). Fast and slow gating behavior of single Ca channels in cardiac cells. *Pflügers Archiv* **406**, 241–258.

CHAD, J. E. & ECKERT, R. (1984). Ca domains associated with individual currents can account for anomalous voltage relations of Ca-dependent responses. *Biophysical Journal* **45**, 993–999.

DEFELICE, L. J., GOOLSBY, W. N. & HUANG, D. (1985). Membrane noise and excitability. In *Noise in Physical Systems*, ed. D'AMICO, A. & MAZZETTI, P., pp. 35–45. Elsevier, Amsterdam.

FISCHMEISTER, R. & HORACKOVA, M. (1983). Variation of intracellular Ca following Ca current in heart. *Biophysical Journal* **41**, 341–348.

FUJII, S., AYER, R. K. & DEHAAN, R. L. (1988). Development of the fast Na current in early embryonic chick heart cells. *Journal of Membrane Biology* **101**, 209–223.

HAGIWARA, S. & NAKAJIMA, S. (1966). Effects of intracellular Ca concentrations upon the excitability of the muscle fiber membrane of a barnacle. *Journal of General Physiology* **49**, 807–818.

HARTZELL, H. C. & WHITE, R. W. (1989). Effects of Mg on inactivation of the voltage-gated Ca current in cardiac myocytes. *Journal of General Physiology* **94**, 745–767.

HESS, P., LANSMAN, J. B. & TSIEN, R. W. (1984). Different modes of Ca channel gating behavior favoured by dihydropyridine Ca agonists and antagonists. *Nature* **311**, 538–544.

HESS, P., LANSMAN, J. B. & TSIEN, R. W. (1986). Ca channel selectivity for divalent and monovalent cations. *Journal of General Physiology* **88**, 293–319.

HESS, P. & TSIEN, R. W. (1984). Mechanism of ion permeation through Ca channels. *Nature* **309**, 453–456.

HIRANO, Y., JANUARY, C. T. & FOZZARD, H. A. (1989). Characteristics of L and T Ca currents in canine cardiac Purkinje cells. *American Journal of Physiology* **256**, H1478–1492.

HUME, J. R. & GILES, W. (1983). Ionic currents in single isolated bull frog atrial cells. *Journal of General Physiology* **81**, 153–194.

JOSEPHSON, I. R., SANCHEZ-CHAPULA, J. & BROWN, A. M. (1984). A comparison of Ca currents in rat and guinea-pig single ventricular cells. *Circulation Research* **54**, 144–156.

KASS, R. S. & SANGUINETTI, M. C. (1984). Inactivation of Ca channel current in the calf cardiac Purkinje fiber. Evidence for the voltage- and Ca-mediated mechanisms. *Journal of General Physiology* **84**, 705–726.

KAWANO, S. & DEHAAN, R. L. (1989). Low-threshold current is major calcium current in chick ventricle cells. *American Journal of Physiology* **256**, H1505–1508.

KOHLHARDT, M., KRAUSE, H., KUBLER, M. & HERDEY, A. (1975). Kinetics of inactivation and recovery of the slow inward current in the mammalian ventricular myocardium. *Pflügers Archiv* **355**, 1–17.

LACERDA, A. E. & BROWN, A. M. (1989). Nonmodal gating of cardiac Ca channels as revealed by dihydropyridines. *Journal of General Physiology* **93**, 1243–1273.

LACERDA, A. E., RAMPE, D. & BROWN, A. M. (1988). Effects of protein kinase C activators on cardiac Ca channels. *Nature* **335**, 249–251.

LANSMAN, J. B., HESS, P. & TSIEN, R. W. (1986). Blockade of current through single Ca channels by Cd, Mg, and Ca. *Journal of General Physiology* **88**, 321–347.

LEDERER, W. J., NIGGLI, E. & HADLEY, R. W. (1990). Na–Ca exchange in excitable cells: fuzzy space. *Science* **248**, 283.

LEE, K. S., MARBAN, E. & TSIEN, R. W. (1985). Inactivation of calcium channels in mammalian heart cells: joint dependence on membrane potential and intracellular calcium. *Journal of Physiology* **364**, 395–411.

LUX, H. D. & BROWN, A. M. (1984). Single channel analysis on inactivation of Ca channels. *Science* **225**, 432–434.

MCDONALD, T. F., CAVALIE, A., TRAUTWEIN, W. & PELZER, D. (1986). Voltage-dependence properties of macroscopic and elementary Ca channel currents in guinea-pig ventricular myocytes. *Pflügers Archiv* **406**, 437–448.

MAZZANTI, M. & DEFELICE L. J. (1987*a*). Regulation of the Na-conducting channel during the cardiac action potential. *Biophysical Journal* **51**, 115–121.

MAZZANTI, M. & DEFELICE, L. J. (1987*b*). Na channel kinetics during the spontaneous heart beat in embryonic chick ventricle cells. *Biophysical Journal* **12**, 95–100.

MAZZANTI, M. & DEFELICE, L. J. (1988). K channel kinetics during the spontaneous heart beat in embryonic chick ventricle cells. *Biophysical Journal* **54**, 1139–1148.

MAZZANTI, M. & DEFELICE, L. J. (1990*a*). Ca modulates outward current through IK1 channels. *Journal of Membrane Biology* **116**, 41–45.

MAZZANTI, M. & DEFELICE L. J. (1990*b*). Ca Channel gating during cardiac action potentials. *Biophysical Journal* **58**, 1059–1065.

MENTRARD, D., VASSORT, G. & FISCHMEISTER, R. (1984). Ca-mediated inactivation of the Ca conductance in Cs-loaded frog heart cells. *Journal of General Physiology* **83**, 105–131.

NILIUS, B., HESS, P., LANSMAN, B. & TSIEN, R. W. (1985). A novel type of cardiac Ca channel in ventricular cells. *Nature* **316**, 443–446.

OSAKA, T. & JOYNER, R. W. (1991). Developmental changes in Ca channels of rabbit ventricular cells. *Circulation Research* **68**, 788–796.

OSTERRIEDER, W., BRUM, G., HESCHELER, J., TRAUTWEIN, W., FLOCKERZI, V. & HOFMANN, F. (1982). Injection of cyclic AMP-dependent protein kinase into cardiac myocytes modulates Ca current. *Nature* **298**, 576–578.

PELZER, D., PELZER, S. & MCDONALD, T. F. (1990). Properties and regulation of Ca channels in muscle cells. *Reviews of Physiology Biochemistry and Pharmacology* **114**, 107–207.

PIETROBON, D. & HESS, P. (1990). Novel mechanism of voltage-dependent gating in L-type Ca channels. *Nature* **346**, 651–655.

REUTER, H. (1983). Ca channel modulation by neurotransmitters, enzymes and drugs. *Nature* **301**, 569–574.

REUTER, H., STEVENS, C. F., TSIEN, R. W. & YELLEN, G. (1982). Properties of single Ca channels in cardiac cell culture. *Nature* **297**, 501–504.

ROSENBERG, R. L., HESS, P. & TSIEN, R. W. (1988). Cardiac Ca channels in planar lipid bilayers. *Journal of General Physiology* **92**, 27–54.

TSIEN, R. W., BEAN, B. P., HESS, P. & NOWYCKY, M. C. (1983). Ca channels: Mechanisms of b-adrenergic modulation and on permeation. *Cold Spring Harbor Symposia on Quantitative Biology XLV* (2), 201–212.

TSIEN, R. W., GILES, W. & GREENGARD, P. (1972). cAMP mediates the effects of adrenaline on cardiac Purkinje fibers. *Nature* **240**, 181–183.

WELLIS, D., DEFELICE, L. J. & MAZZANTI, M. (1990). Outward Na current in beating heart cells. *Biophysical Journal* **57**, 41–48.

YUE, D. T., BACKX, P. H. & IMREDY, J. P. (1991). Ca-sensitive inactivation in the gating of single Ca channels. *Science* **250**, 1735–1738.

YUE, D. T., HERZIG, S. & MARBAN, E. (1990). β-Adrenergic stimulation of Calcium channels occurs by potentiation of high-activity gating modes. *Proceedings of the National Academy of Sciences of the USA* **87**, 753–757.

YUE, D. T. & MARBAN, E. (1990). Permeation in the dihydropyridine-sensitive Ca channel: multi-ion occupancy but no mole-fraction effect between Ba and Ca. *Journal of General Physiology* **95**, 911–939.